The Journal of Green Energy and Environmental Engineering

Research Paper

Highly thermally conductive and light-responsive phase-change cellulose film

Ivan kandil [1], Ian Fleming [2,*]

[1] Donostia International Physics Center, BERC Basque Excellence Research Centre, Manuel de Lardizabal 4, Donostia-San Sebastian E-20018, Spain
[2] Chemical and Environmental Engineering Department, Engineering Faculty of Gipuzkoa, University of the Basque Country UPV/EHU, Plaza Europa 1, Donostia 20018, Spain
*Corresponding author: Ian_Fleming@nps.edu

Abstract. Solar energy storage faces numerous challenges, which mainly stem from the intermittency of solar radiation and energy loss caused by uncontrolled spontaneous heat dissipation of conventional phase-change materials (PCMs) under low-temperature environments. On this basis, this study fabricated a novel light-responsive phase-change composite film (EC/mAZO/BNNs) via physical blending of ethyl cellulose (EC), 4-methoxyazobenzene (mAZO) and boron nitride nanosheets (BNNs). Experimental results show that abundant hydroxyl groups in EC form strong hydrogen-bond interactions with mAZO molecules. These interactions not only effectively inhibit premature crystallization of mAZO but also markedly stabilize its supercooled state, thereby achieving long-term energy storage. Ultraviolet charging experiments demonstrate that the EC/mAZO/BNNs film reaches its photostationary state within 15 min, much faster than the 40 min required for pure mAZO, with greatly improved light-response efficiency; its cis-isomer content reaches 96.8 %, far higher than the 75.7 % of pure mAZO. When BNNs are doped at a mass fraction of 20 %, the thermal conductivity of the film rises to 0.74 W/(m·K), approximately ten times that of the EC/mAZO system without BNNs. In addition, this material can efficiently store light energy through dual mechanisms of isomerization enthalpy and phase-change enthalpy, delivering an energy storage density of about 272.5 J/g. Practical application evaluations reveal that the film can rapidly conduct heat generated during the operation of electronic devices. It exhibits broad application prospects in the field of smart-device thermal management and offers a feasible technical route for developing scalable, durable and multi-functional solar-thermal energy storage systems.

Keywords: *Long-term energy storage; azobenzene; ethyl cellulose; boron nitride*

Received on 02 July 2025, Accepted on 05 Nov 2025, Published on 15 Dec 2025

1 Introduction

Solar energy, a clean and renewable energy source, has attracted extensive attention. Nevertheless, its intermittency and instability bring huge challenges to large-scale and continuous applications. Therefore, advanced technologies for solar energy capture, storage and on-demand release need to be developed. At present, thermal-energy-storage (TES) systems based on phase-change materials (PCMs) have been widely studied to resolve this temporal mismatch. Traditional PCMs such as paraffin waxes, polyethylene glycol and fatty acids can store and release latent heat during their solid-liquid phase transition. Despite their high energy density, their energy release is only passively triggered by environmental cooling. This fundamental defect limits their practicality in controllable thermal management.

In contrast, solar thermal fuels based on photochromic molecules (e.g., azobenzene derivatives) can capture solar energy through reversible trans-cis isomerization. Moreover, they can superimpose isomerization enthalpy and phase-change enthalpy via light-induced melting of azobenzene crystals, so as to realize controllable and repeatable energy storage and release. Hence, they are regarded as important candidate materials for achieving controllable light-heat storage. Under ultraviolet irradiation, azobenzene molecules transform from the low-energy trans-configuration to the high-energy cis-configuration and store isomerization enthalpy and phase-change enthalpy. Under visible-light irradiation or other external-energy stimuli, metastable cis-molecules overcome the energy barrier and revert to the trans-form to release stored thermal energy. However, common azobenzene composite materials suffer from short energy-storage duration, low charging efficiency and low thermal conductivity. To extend thermal-energy-storage time, researchers have explored various innovative strategies for stabilizing metastable states. Among them, raising the activation-energy barrier of phase change is a promising approach. For instance, sodium acetate trihydrate was encapsulated in polyacrylamide hydrogel networks. Stable intermolecular hydrogen bonds were formed to stabilize its supercooled state, enabling thermal-energy storage for up to two years at room temperature. Alternatively, high-latent-heat sugar-alcohol phase-change materials were dispersed in polyvinyl-alcohol (PVA)-based ionically cross-linked networks. The unique performance of this system originates from strong intermolecular interactions within the polymer matrix. Such interactions can suppress undesired crystallization of phase-change materials during cooling and induce glass transition instead of direct crystallization. Accordingly, regulating the activation-energy barrier of solid-liquid phase transitions by hydrogen bonds has become an effective strategy for long-term energy storage.

As a natural biopolymer, ethyl cellulose (EC) features excellent film-forming performance, favorable dispersibility and abundant hydroxyl functional groups. It is therefore considered an ideal matrix candidate. These properties enable it to form extensive intermolecular hydrogen bonds with azobenzene compounds, which effectively inhibit their premature crystallization and stabilize metastable structures. Nevertheless, polymer-based composite energy-storage materials generally suffer from low thermal conductivity, which to some extent restricts their applications in high-efficiency thermal management. Especially in electronic-device heat dissipation and fast-response energy-storage systems, internal heat-conduction efficiency directly affects energy-release rate and temperature-regulation capacity. Low thermal conductivity tends to cause heat accumulation and degrade overall system performance. Consequently, improving thermal-conduction performance while preserving energy-storage performance has become one of the key issues in designing composite energy-storage materials. Boron nitride nanosheets (BNNs) are typical two-dimensional inorganic fillers with intrinsic high thermal conductivity, outstanding electrical insulation and good chemical stability. They have been widely adopted in high-thermal-conductivity polymer composites. Their sheet-like structure facilitates building continuous heat-conduction pathways inside polymer matrices, effectively lowering interfacial thermal resistance and boosting the overall thermal conductivity of the system. Therefore, introducing BNNs into light-responsive phase-change energy-storage systems is expected to construct efficient thermal-conducting networks inside composites. Without significantly damaging the original energy-storage structure, thermal-diffusion capacity and energy-transfer efficiency can be enhanced, offering an effective pathway for synergistically optimizing energy-storage and thermal-management performances.

Based on the above background, 4-methoxyazobenzene (mAZO) and BNNs were incorporated into EC film matrices in this study. A multi-functional composite film integrating high photothermal-conversion capacity, long-duration energy-storage characteristics and high thermal-conductivity performance was successfully prepared. This material holds broad application prospects in thermal management for smart electronic devices and is expected to promote technological innovation and sustainable industrial development of related technologies.

2 Materials and Methods

2.1 Experimental Materials

Ethyl cellulose (EC) was purchased from Tianjin Huasheng Chemical Reagent Co., Ltd. mAZO and absolute ethanol were obtained from Macklin Reagent Co., Ltd., all of analytical grade. Boron nitride (BN) powder was

supplied by Sinopharm Chemical Reagent Co., Ltd. Isopropanol (analytical grade) was bought from Aladdin Biochemical Technology Co., Ltd.

2.2 Preparation of Boron Nitride Nanosheets

BN powder was dispersed in a mixture of deionized water and isopropanol at a volume ratio of 1:1. The BN powder suspension was ultrasonicated for 24 h in an ultrasonic cleaner at 300 W. The suspension was first centrifuged at 500 r/min for 10 min. The collected supernatant was further centrifuged at 9 000 r/min for 10 min. The precipitate obtained from the second centrifugation was freeze-dried for 24 h to yield exfoliated BNNs.

2.3 Fabrication of EC/mAZO/BNNs

The fabrication procedure of EC/mAZO/BNNs is illustrated in Figure 1. 0.4 g of EC and 4.6 g of absolute ethanol were weighed into a sample vial and ultrasonicated for 30 min to prepare an 8 mass-% EC absolute-ethanol solution. Meanwhile, 0.325 g of mAZO and BNNs of corresponding mass ratios were weighed for standby application.

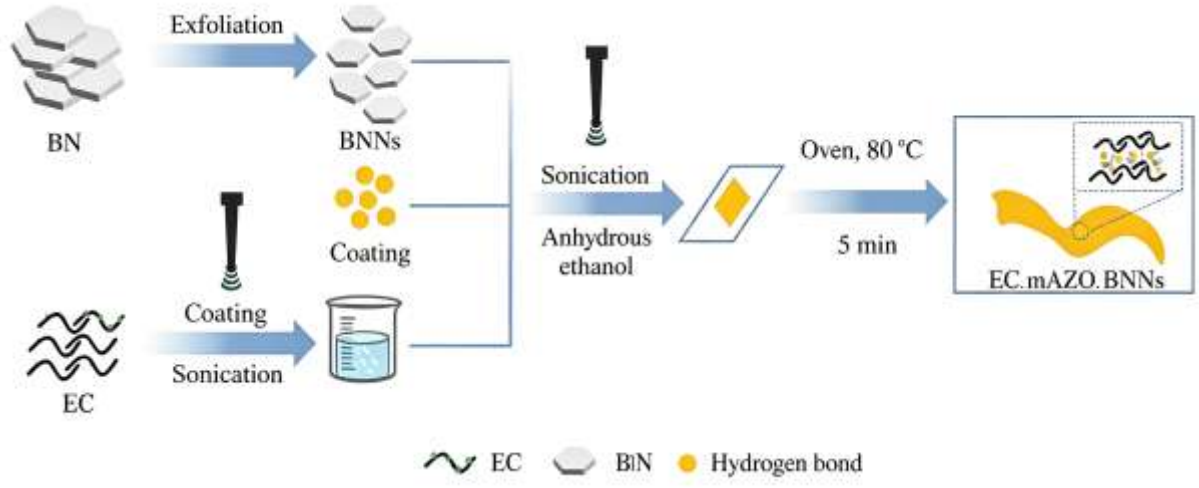

Figure 1 Preparation process of EC/mAZO/BNNs

Table1 Composition ratiosofhigh-thermal-conductivity photoresponsive phase-change films

Sample	EC / g	Anhydrous ethanol / g	mAZO / g	BNNs / g
EC/mAZO/BNNs5	0.48	5.52	0.4	0.046
EC/mAZO/BNNs10	0.48	5.52	0.4	0.098
EC/mAZO/BNNs20	0.48	5.52	0.4	0.220
EC/mAZO/BNNs30	0.48	5.52	0.4	0.380
EC/mAZO/BNNs40	0.48	5.52	0.4	0.590

A magnetic stir bar was placed into the sample vial containing 8 mass-% EC absolute-ethanol solution for magnetic stirring. mAZO and BNNs of corresponding mass fractions were added sequentially. After mAZO was fully dissolved, the mixed solution was ultrasonicated for 30 min and uniformly coated onto polytetrafluoroethylene films. The coated films were placed in an oven at 80 °C for 5 min, and samples were taken out afterwards (average sample thickness: 127.3 μm). Five groups of samples with different component ratios were prepared in parallel (see Table 1 for component ratios). The as-prepared samples were named

high-thermal-conductivity light-controlled phase-change films, denoted as EC/mAZO/BNN*x*, where *x* represents the mass fraction of boron nitride nanosheets. EC/mAZO/BNNs by default refers to composite films with 20 mass-% BNNs. In addition, films of different thicknesses can be obtained by adjusting film-forming processes: after 30 min of ultrasonication, the mixed solution was poured into petri dishes and vacuum-dried in an oven at 35 °C for about 24 h to obtain target samples. Film thickness can be controlled by adjusting solution dosage.

2.4 Characterization of EC/mAZO/BNNs

The chemical structures of samples were characterized by a Nicolet iS20 Fourier-transform infrared spectrometer (FT-IR, Thermo Fisher, USA). A TM3030 scanning electron microscope (SEM, Hitachi, Japan) was adopted to capture micro-surface morphologies of samples. At room temperature, a Lambda 750 ultraviolet-visible spectrophotometer (UV-Vis, PerkinElmer, USA) was used to acquire UV-Vis spectra within the range of 250–600 nm. An MIT500 optical microscope (OM, Aote Optical Instrument Co., Ltd., Chongqing, China) was used to record macro-surface morphologies of samples. A Q20 differential scanning calorimeter (DSC, TA Instruments, USA) was employed to test thermal properties of samples. Tests were conducted under nitrogen atmosphere with a heating rate of 10 °C/min from 0 °C to 150 °C. Photothermal-conversion tests were carried out under irradiation of a PLS-SEX300UV xenon lamp (Bruker, Germany). Temperature variations were acquired by a FLIR E76 infrared imager (IR, Bruker, Germany). The spectral band of the xenon-lamp lens ranged from 200 nm to 2 500 nm, and the lens-to-sample distance was 100 cm. Thermal conductivity of samples was measured by a TPS2500S thermal-constant analyzer (TPS, Hot Disk, Sweden). A STA200 thermogravimetric analyzer (HITACHI, Japan) was used for thermogravimetric analysis. Tests ran from 25 °C to 800 °C at a heating rate of 10 °C/min under nitrogen atmosphere. Mechanical performances of strip-shaped samples were evaluated by a UTM2503 universal testing machine (Sansi Zongheng, China).

2.5 Calculation of Energy-Storage Density

Combining phase-change latent heat and isomerization enthalpy, the overall energy density of EC/mAZO/BNNs composites under different doping ratios can be calculated via Formula (1):

$$\Delta H_{storage} = \Delta H_{cryst} + \Delta H_{iso}$$

where Δ H torage is the total enthalpy change during energy storage, J/g; Δ H cryst is the enthalpy change during crystallization, J/g; Δ H iso is the enthalpy change during isothermal process, J/g.

2.6 Calculation Parameters Related to Photoisomerization

In formula derivation, mAZO in dilute solution at photostationary state is approximately regarded as 100 % cis-configuration. The cis-isomer content c_{is} is calculated by Formula (2):

$$c_{is} = (A - A_i)/(A_c - A_i) \times 100\% \qquad (2)$$

where A is the absorbance at the pi-pi* transition absorption band at a certain moment during trans-to-cis photoisomerization of samples; Aiis the absorbance of samples at the initial state; Ac is the absorbance for 100 % cis-configuration of samples (calibrated by the limit value of complete conversion of mAZO in absolute ethanol solution at photostationary state).

The thermal-relaxation behavior of mAZO follows first-order kinetics Kr:

$$\ln[(A_\infty - A_t)/(A_\infty - A_0)] = -K_r \qquad (3)$$

where A0 is the absorbance of trans-isomer; Ax is the absorbance of cis-isomer; At is the absorbance of samples at time *t*; Kr is the first-order reaction-rate constant reflecting the cis-to-trans isomerization rate, s^{-1}. A larger Kr value indicates faster cis-trans isomerization rate, and vice versa.

Substituting Kr into the formula yields the storage half-life tau1/2 of mAZO:

$$\tau_{1/2} = \ln 2 / K_r \qquad (4)$$

Furthermore, the thermal barrier Ea of reversal process can be calculated by Formula (5):

$$E_a = RT \ln(h \ln 2 / \tau_{1/2} k_B T) \qquad (5)$$

where *T* is storage temperature, K; tau1/2 is storage half-life, h; kB, *R* and *h* represent Boltzmann constant, gas constant and Planck constant respectively.

3 Results and Analysis

3.1 Physicochemical Properties and Micro-Morphology Analysis

In this study, novel high-thermal-conductivity light-controlled phase-change films EC/mAZO/BNNs were fabricated by compounding hydroxyl-rich ethyl cellulose with 4-methoxyazobenzene and boron nitride nanosheets. The first step of the thermal-storage cycle is for trans-crystalline composite films (EC/trans-c-mAZO/BNNs). Under ultraviolet irradiation, trans-c-mAZO molecules in the system absorb photon energy and undergo photoisomerization from trans-configuration to cis-configuration. Meanwhile, accompanied by phase-state variation of molecules, materials transform from original ordered crystalline state to disordered amorphous state, finally forming high-energy metastable EC/cis-m-mAZO/BNNs. During this process, mAZO molecules convert absorbed light energy into chemical energy Δ H isom stored in molecular structures. At the same time, crystal destruction corresponding to phase-state change is accompanied by absorption of phase-change energy Δ H cryst, thus realizing synergistic storage of light energy into multiple forms of energy. Afterwards, under visible-light irradiation, cis-m-mAZO molecules in the system undergo reverse isomerization, reverting from high-energy cis-configuration back to low-energy trans-configuration (trans-m-mAZO) and releasing chemical energy Δ H iso stored in molecules, completing controllable energy release. Notably, ethyl cellulose plays a vital regulatory role in this composite system. Abundant hydroxyl groups on its molecular chains can interfere with ordered arrangement of mAZO molecules via steric-hindrance effects and dipole-dipole interactions. It can also restrict molecular migration to a certain extent, effectively inhibiting regular stacking and crystallization of trans-m-mAZO. Therefore, a long-term supercooled state can be maintained under trans-configuration to avoid premature release of stored energy. In addition, experimental results show that under external mechanical stimuli, molecular systems in supercooled or disordered states can acquire extra energy to overcome activation-energy barriers for transformation from disordered state to crystalline state. This induces rapid crystallization of the system and releases corresponding phase-change energy, finally restoring to stable crystalline state (EC/trans-c-mAZO/BNNs) and completing one full energy-storage cycle. This cycle can be observed by optical microscopy, as shown in Figure 2a.

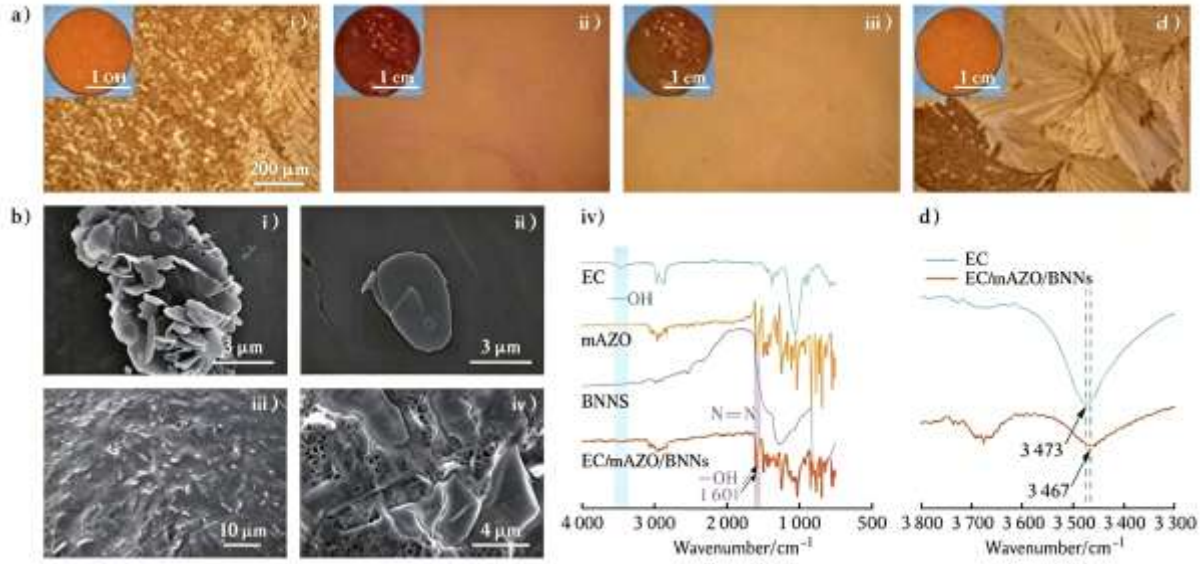

Figure 2 M orphology characterization im agesofEC/m AZO/BNNscom posites

From micro-structures under electron microscopy (Figure 2b), treated BNNs (i) exhibit single-layer sheet-like morphology, which facilitates more uniform dispersion in films and effectively suppresses agglomeration. Meanwhile, mAZO is homogeneously distributed in matrices, which helps guarantee consistency and stability of optical and thermal-conductivity performances of composites. From FT-IR spectra (Figure 2c), EC/mAZO/BNNs spectra display characteristic N=N peaks of mAZO (1 579 cm^{-1} and 1 601 cm^{-1}), proving successful introduction of mAZO into EC. From Figure 2d, the O-H absorption peak of EC/mAZO/BNNs appears at 3 467 cm^{-1}, showing blue shift and peak broadening compared with the O-H absorption peak (3 473 cm^{-1}) of pure EC. This confirms hydrogen-bond formation between EC and mAZO. Besides, no new peaks beyond characteristic-peak ranges of EC, mAZO and BNNs emerge in EC/mAZO/BNNs spectra. It indicates that EC, mAZO and BNNs form structurally stable composite systems through physical interactions, laying reliable micro-structural foundations for excellent light-responsiveness, long-term energy-storage characteristics and high-efficiency thermal-conductivity performances of composites.

3.2 Thermal-Conductivity Performance Analysis

Thermal conductivity (*k*) is a key property for evaluating efficiency of thermal-interface materials (TIMs). As shown in Figure 3a, thermal-conductivity increases gently in the low-filler region because boron nitride nanosheets are embedded in EC networks as dispersed phases. Thermal conductivity of composites keeps rising with increasing mass fraction of BNNs. Notably, when the mass fraction of BNN fillers reaches 20 %, the *k* value of EC/mAZO/BNNs composites attains 0.74 W/(m·K), which is 1 038 % higher than 0.065 W/(m·K) of EC/mAZO. At this point, BNNs have formed spatially interconnected thermal-conducting skeletons (Figure 2b). After multiple thermal cycles, thermal conductivity of EC/mAZO/BNNs barely changes (Figure 3b), demonstrating stable thermal-conductivity of composite films after repeated thermal cycles. To further verify superior heat-transfer performance of EC/mAZO/BNNs, comparative heating experiments were performed to assess thermal performances of EC/mAZO/BNNs and EC/mAZO, as shown in Figures 3c-d.

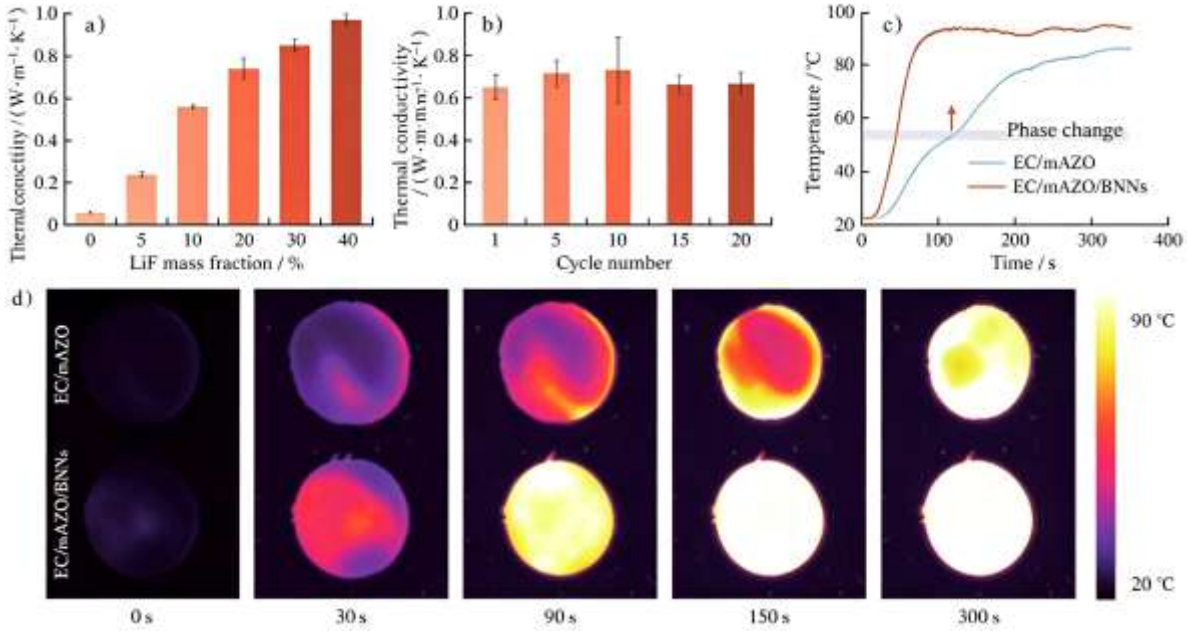

Figure 3 Thermal conductivity of EC/mAZO/BNNs composites

Surface temperature of samples rises gradually and stabilizes after approximately 150 s. The surface-heating rate of EC/mAZO/BNNs is obviously higher than that of EC/mAZO. It is worth noting that near the identical phase-change temperature (about 52.5 °C), heating rates of EC/mAZO/BNNs and EC/mAZO decrease significantly due to heat absorption during phase-change processes, showing a short stable period lasting for around 10 s. In practical applications, such behavior effectively eliminates thermal shock of electronic devices during rapid heating. At steady state, the surface temperature of EC/mAZO/BNNs is close to heater temperature and about 10 °C higher than that of EC/mAZO, which originates from higher thermal conductivity of EC/mAZO/BNNs. The high thermal conductivity and outstanding thermal-conductivity stability exhibited by EC/mAZO/BNNs composites jointly guarantee thermal-conducting reliability during long-term service, endowing them broad application potential in light-controlled energy-storage and intelligent thermal-management fields.

3.3 Energy-Storage Performance Analysis

Energy density of EC/mAZO/BNNs composites consists of two parts: one is phase-change enthalpyΔ Hpc of trans-mAZO, and the other is energyΔHiso released during cis-trans isomerization of cis-mAZO molecules. DSC curves of pure mAZO after ultraviolet charging (Figure 4a) show that pure cis-molten-state mAZO presents broad peaks within 60–130 °C. These peaks are generated by photoisomerization of cis-molten-state mAZO to trans-molten-state mAZO ΔHiso.

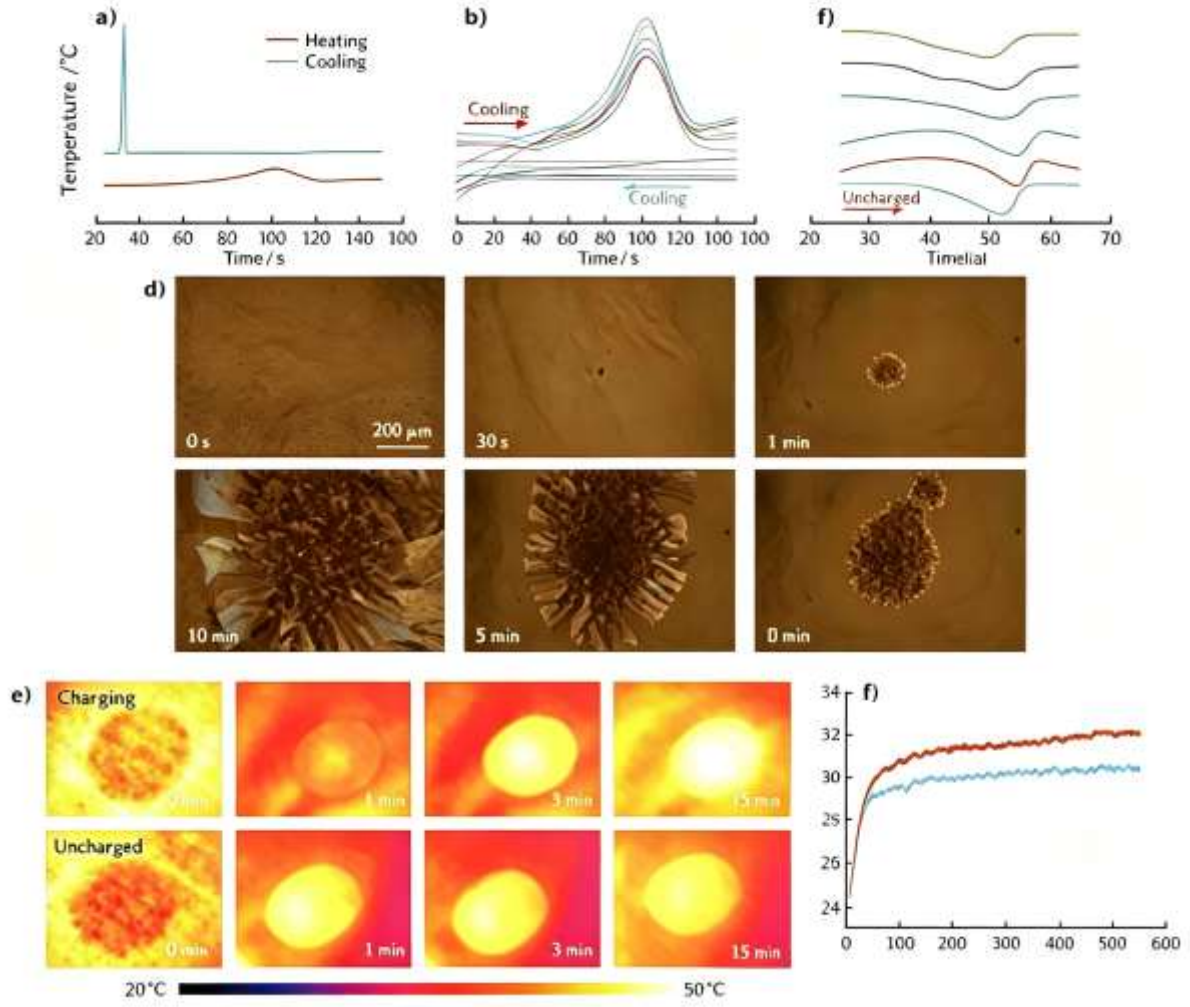

Figure 4 Energy storage performance of EC/m AZO/BNNs composites

When temperature drops to 34 °C, crystallization transition to trans-crystalline-state mAZO occurs, releasing phase-change energy Δ Hcrys. From DSC heating curves of composites with different BNNs additions after ultraviolet charging (Figure 4b), all samples show broad peaks within 60-130 °C after charging. Then temperature decreases to 0 °C, and dopant mAZO remains molten. This phenomenon can be attributed to extensive hydrogen-bond networks formed between hydroxyl groups on EC molecules and mAZO. Therefore, movement of mAZO molecules in EC/mAZO/BNNs composites is greatly restricted. They cannot spontaneously re-form closely packed crystal structures, so stable long-term energy storage is realized. Heat stored in supercooled EC/trans-m-mAZO/BNNs (ΔHpc≈Δ Hcryst≈Δ Hfus), where Δ Hfus denotes fusion enthalpy) can be released by introducing seed crystals, heating or mechanical stimuli to provide extra energy input. Experimental verification results: EC/mAZO/BNNs was placed in an oven at 90 °C for 5 min and then in a refrigerator at −10 °C for 5 min. At this moment, EC/mAZO/BNNs stays in supercooled state and dopant mAZO remains molten. When composite films are taken out of the refrigerator, crystallization of dopant mAZO takes place. This process can be observed via optical microscopy (Figure 4d).

Table2 The energy density of EC/mAZO/BNNs composites with different doping ratios

Mass fraction of BNNs / %	Δ H iso/ ($J \cdot g^{-1}$)	Δ H cryst/ ($J \cdot g^{-1}$)	Δ Hstorage/ ($J \cdot g^{-1}$)	Total Δ H/ ($J \cdot g^{-1}$)
5	91.6	19.69	111.3	257.7

10	87.5	16.34	103.8	253.7
20	86.1	12.98	99.1	272.5
30	76.2	10.60	86.8	272.8
40	63.0	9.27	72.3	265.1

Specific energy-density values of EC/mAZO/BNNs composites with different boron-nitride-nanosheet doping ratios are listed in Table 2. These results indicate that increasing mass fraction of boron nitride nanosheets reduces energy-storage density of EC/mAZO/BNNs.

Energy released by composite films throughout exothermic processes can be verified by infrared thermal imaging and temperature-time curves (Figures 4e and 4f). The surface temperature of charged EC/mAZO/BNNs films is about 1-5 °C higher than that of uncharged films. Such temperature rise mainly originates from release of stored isomerization energy and partial phase-change energy. During testing, contact between films and supporting platforms induces partial crystallization of mAZO components and triggers release of corresponding phase-change enthalpy. After comprehensively considering key factors including thermal conductivity and energy-storage density, EC/mAZO/BNNs with 20 mass-% boron-nitride-nanosheet doping was finally selected as the research system for subsequent photoisomerization-performance studies. Under this filler-addition amount, the unit energy-storage density Δ Hstorage of composites reaches 272.5 J/g, obviously higher than 201.0 J/g of pure mAZO. This result is closely related to high photoisomerization conversion degree in EC/mAZO/BNNs systems, demonstrating that composite structures exert certain promoting effects on molecular photoresponse behaviors, so higher energy-storage capacity is achieved on per-mass scale. In addition, repeated charge-discharge cycle tests for materials reveal that after 10 consecutive charge-discharge cycles, energy-storage density of EC/mAZO/BNNs composite films basically remains consistent with initial test results without obvious attenuation. It proves that materials possess favorable structural stability and energy-storage-performance retention during cycling, and can satisfy performance requirements under repeated-use conditions.

3.4 Photoisomerization Analysis

3.4.1 Ultraviolet-Light Charging Analysis

UV-Vis absorption spectra were utilized to investigate photoisomerization of mAZO and EC/mAZO/BNNs induced by ultraviolet or visible light. mAZO exhibits prominent pi-pi* transition absorption peak near 330 nm (Figure 5a), while a weak pi-pi* transition absorption band appears around 450 nm. With proceeding ultraviolet irradiation, intensity of the pi-pi* absorption band gradually decreases accompanied by blue shift. Meanwhile, intensity of the pi-pi* absorption band keeps increasing with slight blue shift. Such variations mainly stem from photoisomerization transformation of mAZO from trans-configuration to cis-configuration. Under ultraviolet irradiation, photoisomerization reactions of azobenzene reach a dynamic equilibrium state, namely photostationary state (PSS). Under this steady state, cis-isomer content reaches its maximum value and no longer rises with prolonged illumination time. By comparing Figure 5a and Figure 5b, pure mAZO attains photostationary state after 40 min of ultraviolet-lamp irradiation, which is 2.6 times the irradiation time (15 min) required for EC/mAZO/BNNs to reach PSS. This is because uniform dispersion of mAZO in composite films significantly enlarges its effective contact area with incident light, thereby improving light-response efficiency and shortening time required to reach photostationary state. Relative content of cis-mAZO at photostationary state can be estimated by percentage variations of absorbance at the pi-pi* absorption peak. Since ethanol solutions provide high conformational freedom for mAZO molecules, cis-isomer proportions usually exceed 95 % after ultraviolet irradiation. The relationship between ultraviolet-irradiation time and cis-isomer proportion of samples is presented in Figure 5c. Under identical ultraviolet-irradiation duration, EC/mAZO/BNNs materials possess higher cis-isomer proportion, indicating faster charging rate than pure mAZO. Moreover, when EC/mAZO/BNNs composites are irradiated by ultraviolet light to photostationary state, cis-isomer proportion

reaches 96.8 %, remarkably higher than 75.7 % of pure mAZO. High conversion ratio mainly originates from uniform dispersion of mAZO in EC/mAZO films, which enlarges light-illumination contact area and shortens charging time, conducive to improving light-energy-utilization efficiency. These results demonstrate that EC helps improve dispersion state of mAZO and boost its charging rate, and endows composite films with stronger isomerization-energy-storage capacity.

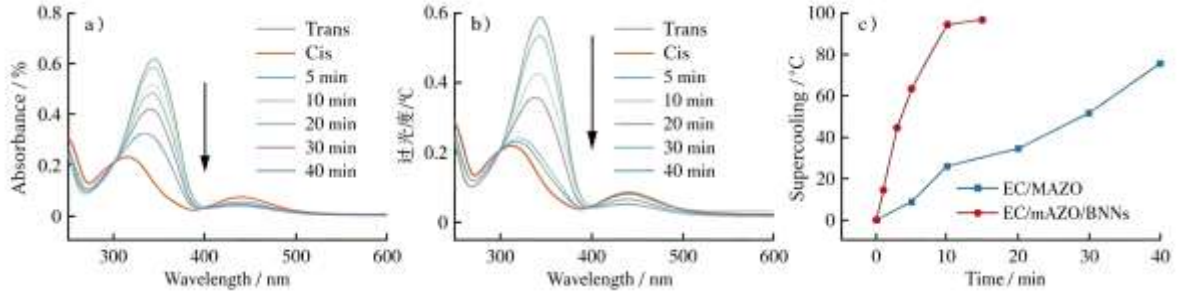

Figure 5 Isomerization performance of EC/mAZO/BNNs composites under UV light

3.4.2 Energy-Release Analysis in Darkness

mAZO exhibits spontaneous reversion behavior under room-temperature dark conditions, i.e., transition from cis-mAZO to trans-mAZO (Figure 6a). Under dark conditions, Kr of EC/mAZO/BNNs and mAZO are 3.82×10^{-6} s^{-1} and 6.72×10^{-6} s^{-1} respectively. EC/mAZO/BNNs features lower Kr, longer tau1/2 and higher Ea. It releases energy more slowly and can store energy for longer periods. This is attributed to hydrogen bonds formed between EC and mAZO, which raise energy barriers during molecular isomerization and effectively prolong energy-storage time. It indicates that EC/mAZO/BNNs owns more stable long-term energy-storage capacity than mAZO.

Values of Kr, tau1/2 and Ea for EC/mAZO/BNNs and mAZO are summarized in Table 3. Calculated from data in Table 3, charged mAZO can completely release energy Δ Hstorage (including Δ Hcryst and ΔHiso in approximately 57.3 h. In contrast, charged EC/mAZO/BNNs can fully release only isomerization energy Δ Hiso in about 100.8 h.

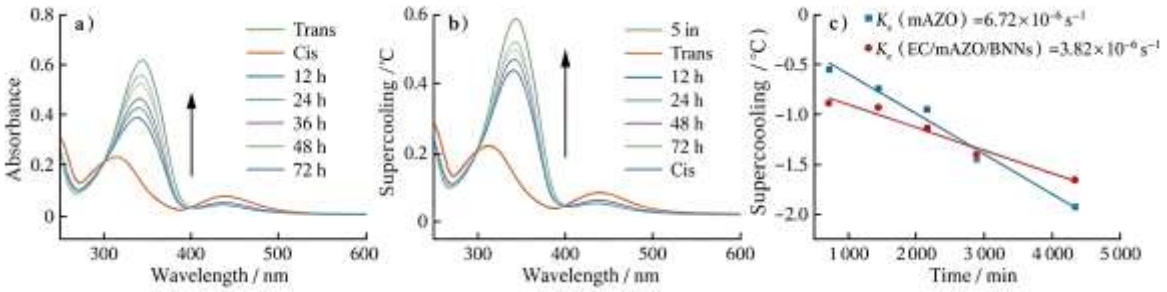

Figure 6 Isomerization performance of EC/mAZO/BNNs composites under dark conditions

3.4.3 Energy-Release Analysis under Blue-Light and Solar Irradiation

Although slow reversion reduces heat loss during storage, heat release controlled by external effects (light, heat or chemicals) under different time or environmental conditions is critical for mAZO serving as solar thermal fuel. According to UV-Vis absorption spectra of EC/mAZO/BNNs under blue-light and sunlight irradiation (Figures 7a and 7b), cis-mAZO can convert back to trans-mAZO. Kr of EC/mAZO under blue-light irradiation is higher than Kr of EC/mAZO/BNNs under sunlight irradiation (Figure 7c). It demonstrates that reversion rate of EC/mAZO/BNNs rises significantly under blue-light irradiation, and full reversion to trans-state can be accomplished within 15 min. Such accelerated reversion of cis-to-trans transformation arises because metastable mAZO absorbs certain amount of energy from light, which is sufficiently high to surmount thermal barrier Ea.

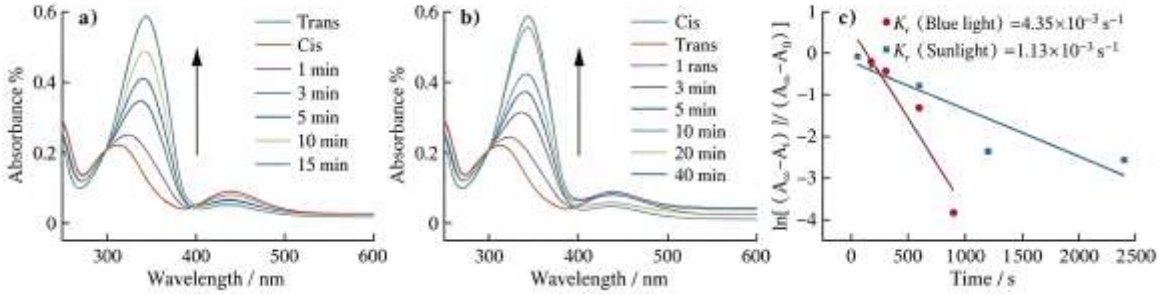

Figure 7 Isomerization performance of EC/mAZO/BNNs composites under visible light

3.5 Stability Analysis

Cycle-performance evaluations were carried out to investigate long-term-service stability of EC/mAZO/BNNs composites. Tensile stress-strain curves of EC/trans-c-mAZO/BNNs and EC/cis-m-mAZO/BNNs are shown in Figure 8a. The trans-crystalline state achieves high strength and high modulus through rigid bearing of ordered crystal lattices; the cis-molten-state realizes high ductility and high toughness via high flowability of amorphous phases. The difference between them essentially originates from distinction of long-range order instead of merely molecular configurations, laying key experimental foundations for industrial applications of light-responsive intelligent composite materials. From thermogravimetric curves of EC/mAZO/BNNs and its respective components (Figure 8b), main thermal-decomposition interval of EC concentrates at 270-395 °C. Decomposition of mAZO takes place within 140-260 °C. By contrast, BNNs show almost no obvious mass loss across the whole test-temperature range and maintain high stability even at 800 °C. For EC/mAZO/BNNs composite systems, thermal decomposition presents typical two-stage characteristics: the first stage (roughly 140-290 °C) mainly corresponds to volatilization and decomposition processes of mAZO; the second stage (290-395 °C) is ascribed to thermal-cracking behavior of EC molecular chains. Overall, decomposition temperatures of EC/mAZO/BNNs composites are distinctly higher than their phase-change-temperature ranges, proving favorable thermal stability of the system during energy-storage and energy-release processes. During five consecutive cycles, absorbance of composite films stays nearly constant without remarkable fluctuations (Figure 8c). It suggests that EC/mAZO/BNNs undergo no significant photodegradation after multiple photoisomerization conversions and possess excellent cycle stability. In addition, observations after ultraviolet-light irradiation of composite films reveal that they can still maintain complete and clear snowflake-shaped structures without obvious leakage (Figure 8d). It indicates that mAZO is effectively confined inside EC matrices, endowing materials favorable anti-leakage performance. In summary, EC/mAZO/BNNs composites integrate good mechanical properties, excellent thermal stability, outstanding cycle stability and favorable anti-leakage capacity, which provide solid support for safety and reliability in practical applications.

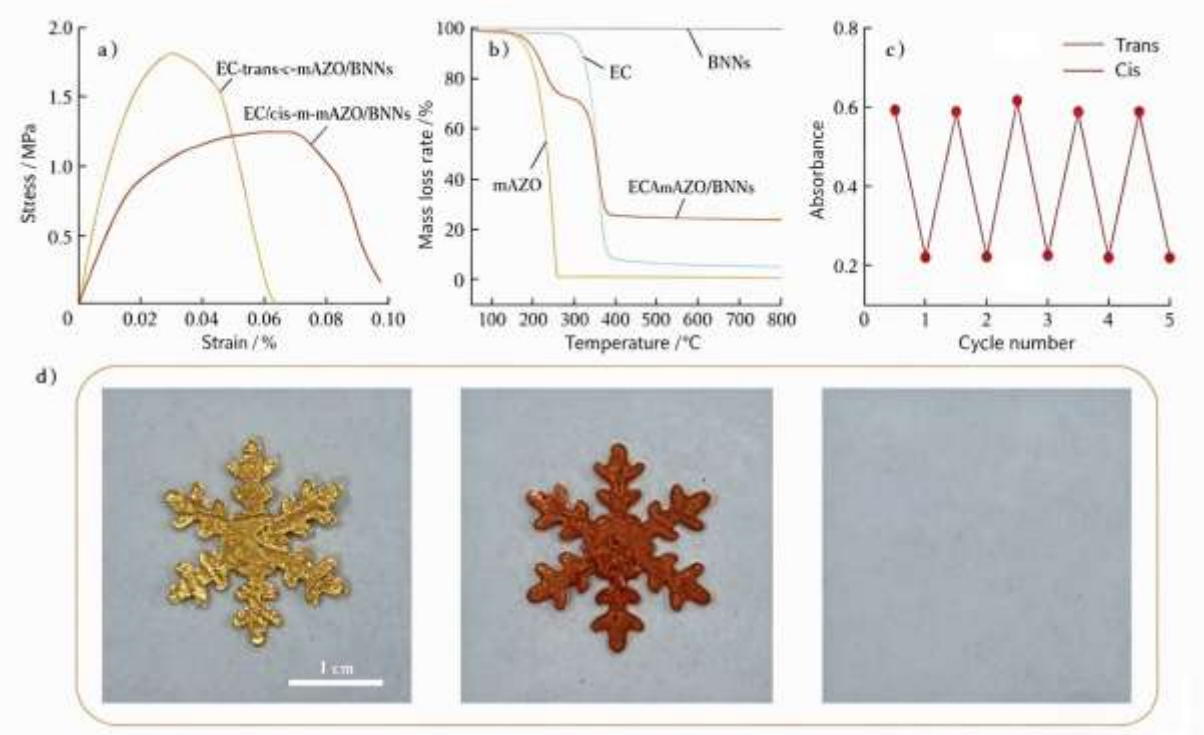

Figure 8 Stability of EC/mAZO/BNNs

3.6 Thermal-Management Applications

To evaluate thermal-management performances, thermal-conduction simulation experiments were conducted. EC/mAZO/BNNs composites were adopted as thermal-interface materials (TIMs) applied to computer CPUs to comprehensively assess their heat-dissipation efficiencies (Figure 9a). Appropriate-sized TIMs were placed at the interface between CPU upper surfaces and fan-radiator bases. Under full-load operating conditions of computers, temperature variations were monitored in real time by dedicated software combined with infrared thermal imagers (Figure 9b). Results show that heat-dissipation systems integrated with EC/mAZO/BNNs reach a steady-state temperature of 44.8 °C within 3 300 s, distinctly higher than 40.8 °C measured for EC/mAZO radiators without boron-nitride-nanosheet additions. Such temperature difference demonstrates that EC/mAZO/BNNs possess superior thermal-conductivity performances and realize more efficient heat transfer from chips to radiators. Meanwhile, their phase-change components feature reversible thermal-energy-storage capacity, which can temporarily store partial waste heat in latent-heat form to collaboratively improve thermal-management efficiency. Higher surface temperature reflects lower interfacial thermal resistance and stronger heat-transfer capacity, which helps promote overall heat-dissipation efficiency. To further clarify performance advantages, comparative analysis of three configurations including EC/mAZO/BNNs, EC/mAZO and blank (without TIM) was performed (Figure 9c). Under identical full-load conditions, CPU temperature rise reaches only 0.5 °C when EC/mAZO is used. Temperature rise further increases upon adoption of EC/mAZO/BNNs composites, proving its stronger heat-export capacity and helping fans release heat to surroundings more rapidly. Such remarkable temperature difference fully validates outstanding heat-transfer performances and temperature-stabilization capacities of EC/mAZO/BNNs composites in thermal-management applications.

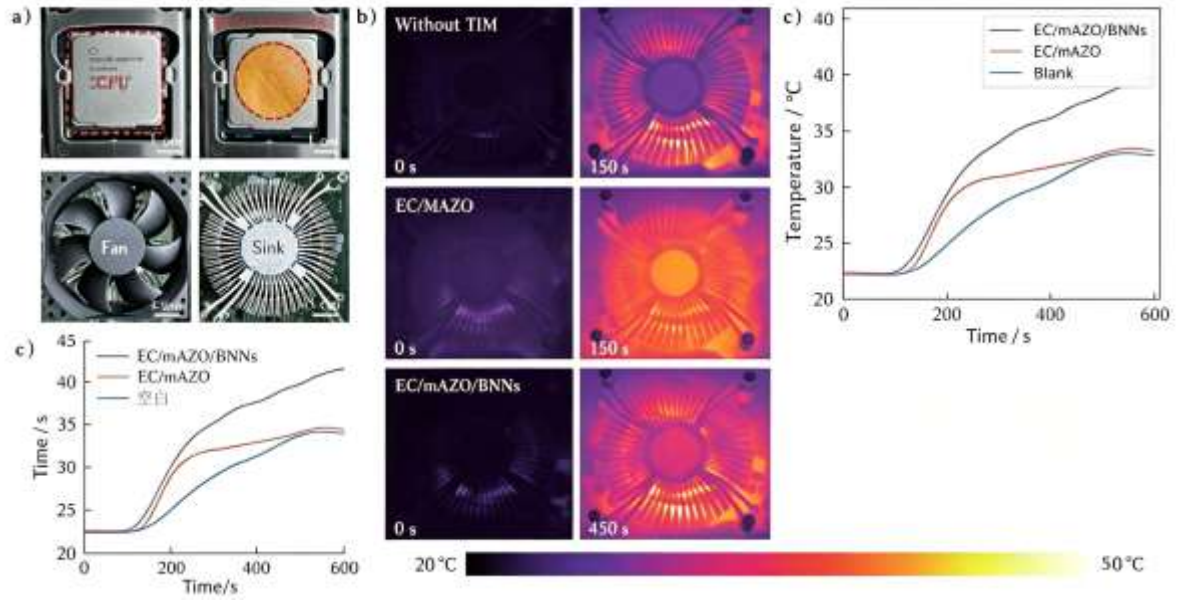

Figure 9 Thermal management performance of EC/mAZO/BNNs composite

4 Conclusions

EC/mAZO/BNNs composite films prepared in this study exhibit excellent long-term energy-storage and on-demand energy-release capabilities, and maintain reliable thermal-conductivity and photoisomerization stability during long-period cycles. Specific conclusions are as follows:

Strong hydrogen-bond interactions between EC and mAZO effectively inhibit crystallization of mAZO and markedly stabilize its supercooled state, achieving long-term energy storage. Stored energy can be released on demand via external stimuli, presenting high-efficiency photothermal-energy-conversion capacity.

EC/mAZO/BNNs composite films reach photostationary state within 15 min (remarkably faster than the 40 min required for pure mAZO), and cis-isomer content is as high as 96.8 %. When 20 mass-% BNNs are doped into films, thermal conductivity rises to 0.74 W/(m·K), approximately 1 038 % higher than EC/mAZO systems without BNNs. In addition, this material stores light energy through dual mechanisms of isomerization enthalpy and phase-change enthalpy together with high isomerization ratio, realizing a high unit energy-storage density of about 272.5 J/g.

Overall, such composite films integrate high photothermal-conversion efficiency, enhanced thermal-conductivity performances and stable energy-storage characteristics. They possess broad application prospects in fields such as light-controlled energy storage and heat-dissipation management for intelligent electronic devices.

References

[1] Aliqab K, Han B B, Kumar O P, et al. Graphene metamaterial solar absorber using Al-TiN-Fe for efficient sol ar thermal energy conversion and optimization using machine learning [J]. Scientific Reports, 2024, 14: 31 643. DOI:10.1038/s41598024-80485-0.

[2] Gao Z M, Boudreaux P, Shabtay Y, et al. Novel thermal energy storage component: development, perform ance, and phase transition diagnosis[J]. Energy Conversion and Management, 2026, 348:120682. DOI:10.1 016/j.enconman.2025.120682.

[3] Wei Y H, Li J J, Sun F R, et al. Leakage-proof phase change composites supported by biomass carbon aerog els from succulents [J].Green Chemistry,2018,20(8): 1858-1865.DOI:10. 1039/c7gc03595k.

[4] Xie H W, Ren Z P, Zhang Y, et al. Enhanced thermal properties of biochar-based shape-stabilized phase ch ange materials for thermal energy storage through $ZnCl_2$ modification [J].Journal of Energy Storage,2026, 143:119649.DOI:10. 1016/j.est.2025.119649.

[5] Lu P, Chen W S, Fan J J, et al. Thermally triggered nanocapillary encapsulation of lauric acid in polystyrene hollow fibers for efficient thermal energy storage[J]. ACS Sustainable Chemistry & Engineering,2018,6(1): 2656-2666.DOI:10. 1021/acssuschemeng.7b04259.

[6] Liu Y Z, Li X X, Xu Y Z, et al. Hydrogel-stabilized supercooled salt hydrates for seasonal storage and controll ed release of solar thermal energy[J].Journal of Materials Chemistry A,2024,12(46): 31982-31992. DOI:10. 1039/d4ta05612d.

[7] Lenert A, Forrest S R. Nexus of solar and thermal photovoltaic technology could help solve the energy stor age problem[J]. Joule,2022,6(6): 1144-1147. DOI:10.1016/j.joule.2022. 05.015.

[8] Liu H, Tang J W, Dong L Q, et al. Optically triggered synchronous heat release of phase-change enthalpy a nd photothermal energy in phase-change materials at low temperatures [J]. Advanced Functional Materia ls,2021,31(6): 2008496. DOI:10.1002/adfm .202008496.

[9] Aftab W, Usman A, Shi J M, et al. Phase change material-integrated latent heat storage systems for sustai nable energy solutions[J].Energy & Environmental Science,2021,14(8): 4268-4291. DOI:10.1039/d1ee005 27h.

[10] Sert S, Ayranci R, Çılgı G K, et al. Photoresponsive conductive polymer network based on azobenzene brid ging crosslinked polycarbazole for boosting solar thermal storage[J].Solar Energy Materials and Solar Cell s, 2024, 278: 113184. DOI:10.1016/j.solmat.2024.113184.

[11] Chen J, Kou Y, Zhang S H, et al. Spatiotemporal utilization of latent heat in erythritol-based phase change materials as solar thermal fuels[J]. Angewandte Chemie International Edition, 2024,63(16): e202400759. DOI:10.1002/anie.202400759.

[12] Yazdani M R, Etula J, Zimmerman J B, et al. Ionic cross-linked polyvinyl alcohol tunes vitrification and col d-crystallization of sugar alcohol for long-term thermal energy storage[J]. Green Chemistry, 2020, 22 (16): 5447- 5462. DOI:10.1039/d0gc01427c.

[13] Horvat G, Žvab K, Knez Ž. Simple,one-pot method for preparing transparent ethyl cellulose films with goo d mechanical properties[J]. Polymers,2022,14(12):2399.DOI:10.3390/polym14122399.

[14] Zhang R H, Sun B J, Chen L Y, et al. An ethyl cellulose-coated bacterial cellulose based hydrophobic and de gradable straw-like materials towards drinking straws[J]. Carbohydrate Polymers, 2025, 367: 124046. DOI: 10.1016/j.carbpolymers.2025.124046.

[15] Xie J L, Tang A, Wang C K, et al. Thermal conductivity analysis of BN/Al_2O_3/TPU composite materials with 3 D printing filler oriented structure[J]. Mechanical Engineer,2025 (12): 62- 66. DOI:10.3969/j. issn. 1002- 2 333. 2025.12.013.

[16] Chen G S, Liu T, Wang Z F, et al. Fabrication and thermal-conductivity study of flexible tear-resistant self-h ealing polyurethane/boron nitride laminated composites[J]. Acta Polymerica Sinica,2025,56(12): 2418-24 29.DOI:10.11777/j.issn.1000-3304.2025.25222.

[17] Sun J G, Wu L, Liu Y, et al. Preparation and properties of waterborne epoxy resin composite coatings with high thermal conductivity and anticorrosion[J]. Thermosetting Resin, 2025, 40(4): 23-27. DOI:10.13650/j.c nki.rgxsz.2025.04.009.

[18] Dong L Q, Zhai F, Wang H, et al. An azobenzene-based photothermal energy storage system for co-harves ting photon energy and low-grade ambient heat via a photoinduced crystal-to-liquid transition[J]. Energy Materials,2022,2(4):200025. DOI:10.10517/energymater.2022.26.

[19] Xu X T, Xing Y M, Yin Y J, et al. Flexible wearable fabrics for solar thermal energy storage and release in o n-demand environments[J]. Chemical Engineering Journal,2023,466: 143175. DOI:10.1016/j.cej.2023.143 175.

[20] Li J, Liu K Y, Wang H, et al. Energy storage and release in optically controlled azobenzene and wood comp osite phase change materials[J].Journal of Northeast Forestry University,2026, 54(3): 1-9. DOI:10.13759/j. cnki.dlxb.2026.03.002.

[21] Cao D X, Li Q, Sun X, et al. Amphipathic binder integrating ultrathin and highly ion-conductive sulfide mem brane for cell-level high-energy-density all-solid-state batteries[J]. Advanced Materials, 2021, 33 (52): 210 5505. DOI:10. 1002/adma.202105505.

[22] Zhao Y L, Liu B Q, Li S L. High thermal conductivity hyperbranched boron nitride/nanocellulose composite films: interface engineering and performance regulation[J/OL]. Transactions of China Electrotechnical Soc iety,1-10[2026-04-07]. https://doi.org/10.19595/j.cnki.1000-6753.tces.251241.

[23] Wang H, Liu K Y, Zhang K, et al. Optically controlled phase change wood for energy storage and heat relea se[J]. Journal of Energy Storage, 2024, 104: 114798. DOI:10.1016/j.est.2024.114798.
[24] Wang H. The synthesis and performance investigation of azobenzene/wood-based phase change energy s torage materials [D].Harbin:Northeast Forestry University,2025.